27th EPS Conference on Contr. Fusion and Plasma Phys. Budapest, 12-16 June 2000 ECA Vol. **24B** *(2000) 241 -244*

Impurity Seeding of JET L–mode Diverted Plasmas with q(0) > 1

G.L. Jackson,[1] M. Brix,[2] R. Budny,[3] C. Challis,*,[4] P. Dumortier,[5] S.K. Erents,[4] N.C. Hawkes,[4] L.D. Horton,*,[6] L.C. Ingesson,*,[4] A. Kallenbach,[6] K.D. Lawson,[4] A. Loarte,*,[7] G. Maddison,[4] G.F. Matthews,*,[4] G.R. McKee,[1] A. Meigs,*,[4] A.M. Messiaen,[5] P. Monier-Garbet,[8] M. Murakami,[1] M.F.F. Nave,[9] J. Ongena,[5] M.E. Puiatti,[10] J. Rapp,[2] G.M. Staebler,[1] J.D. Strachan,[3] B. Unterberg,[2] M. Valisa,[10] and K-D. Zastrow*,[4]

**JET Joint Undertaking, United Kingdom*
[1]DIII–D National Fusion Facility, San Diego, California, USA
[2]IPP-Forschungszentrum, Jülich, Germany
[3]Princeton Plasma Physics Laboratory, Princeton, New Jersey
[4]Euratom/UKAEA Fusion Association, Abingdon, United Kingdom
[5]ERM, Brussels, Belgium
[6]Max-Planck Institute,Garching, Germany
[7]EFDA-CSU Garching, Germany
[8]CEA Cadarache, France
[9]Associação EURATOM/IST, Lisboa, Portugal
[10]Consorzio RFX, Padua

Impurity seeding of plasma discharges has led to regimes of improved thermal and particle confinement in many tokamaks [1]. Extending these results to a larger device such as the JET tokamak allows size scaling and the evaluation of the potential of this approach to future fusion reactors. In the initial JET experiments reported here, neon impurity seeding produced modest increases in thermal energy confinement, $H_{89P} \leqq 1.4$, a reduction in the thermal diffusivity, χ_i, and increases in the thermal neutron rate of more than a factor of 2, accompanied by a large increase in radiated power, $P_{rad}/P_{in} \leqq 0.6$. Gyrokinetic simulation (GKS) code simulations show a decrease in the growth rate of low k modes in discharges with impurity injection, consistent with a reduction in ion temperature gradient (ITG) modes.

Two discharges with neon impurity injection are compared to a reference discharge without neon in Fig. 1. Discharge parameters are similar, I_p=2.5, B_T=3.0 T, q_{95}=4.0. The X–point is above the divertor septum and the outer strike point is positioned for optimal pumping. All discharges maintained an L–mode edge during the time shown. After neon injection [Fig. 1(b)] there is a 0.6 s delay until the radiated power begins increasing. This initial delay is due to the location of the puffing valve which is several meters from the torus. After a further delay, small increases in density and stored energy are also observed [Figs. 1(c) and 1(d)]. Neutral beam power was not constant [Fig. 1(a)], which may account for the delay in the increase of stored energy in discharge #49265 when compared to #49264.

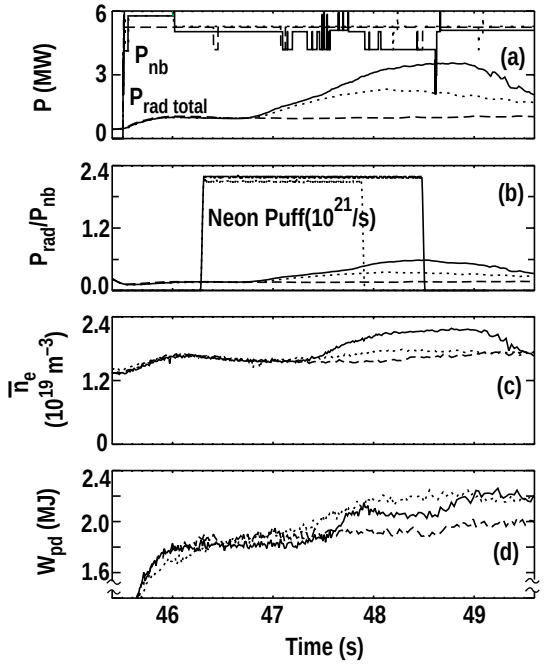

Fig. 1. Impurity injection in two JET discharges, solid (#49265) and dotted (#49264) lines, compared to a reference discharge with no neon (#49270). Discharge parameters are given in the text. Plotted is: (a) neutral beam injected power and total radiated power, (b) neon puff rate and fraction of radiated power, (c) line averaged electron density and (d) diamagnetic stored energy.

The density increase is most pronounced for the discharge with the highest radiated power. The rate of impurity injection is nearly the same in both impurity seeded discharges in Fig. 1 and the initial increases in radiated power are also similar until 47.5 s. After that time, both density and radiated power increase at a faster rate in #49265, perhaps due to lower auxiliary heating power in #49265 which lowered edge electron temperatures which increases radiation efficiency in the mantle region (defined here as $\rho>0.5$).

The TRANSP code [2] has been used to infer transport coefficients for these discharges. Shown in Fig. 2(a) is the ion thermal diffusivity, χ_i, for pulse #49265 with neon seeding and reference discharge #49270 whose temporal behavior was described in Fig. 1. At the end of neon injection, χ_i in the mantle region decreased ~50%. The insets in Fig. 2 show the profiles of χ_i for these discharges at two times: 46.2 and 48.5 s. These profiles are similar at the earlier time, before neon injection in #49265, but χ_i is reduced across the entire profile at the later time. Plasma pressure [Fig. 2(b)] and the thermal neutron rate calculated from TRANSP [Fig. 2(c)] increase after neon injection. Both increases begin in the time interval between the onset of the P_{rad} increase and the beginning of the density rise. Even though there is only a small increase in stored energy, the calculated thermal neutron rate increases more than a factor of 5 in the discharge with neon injection.

The largest change in thermal diffusivity after neon injection is for the ions, which is consistent with results from the DIII–D tokamak [3]. This observation is also consistent with results from the GKS code [4]. Reductions in the growth rates of low k modes, namely ITG modes, after impurity seeding have been identified as the mechanism leading to increases in energy and particle confinement in both DIII–D and TEXTOR [3,5] and this mechanism is a candidate to explain the decreases of χ_i observed in JET discharges. Calculations of the growth rates of microturbulence, γ, as a function of k_θ are displayed in Fig. 3(a). The reference (no neon) discharge shows higher growth rates in the range of k, and frequencies in the ion diamagnetic drift direction [Fig. 3(b)], where ITG mode turbulence is expected. In the discharge with neon seeding γ is reduced over most of this region, but it increases at higher k where the frequency is in the electron diamagnetic drift direction. This is the region where trapped electron modes exist. Although not plotted, γ is nearly zero at even higher k where electron temperature gradient modes would be observed.

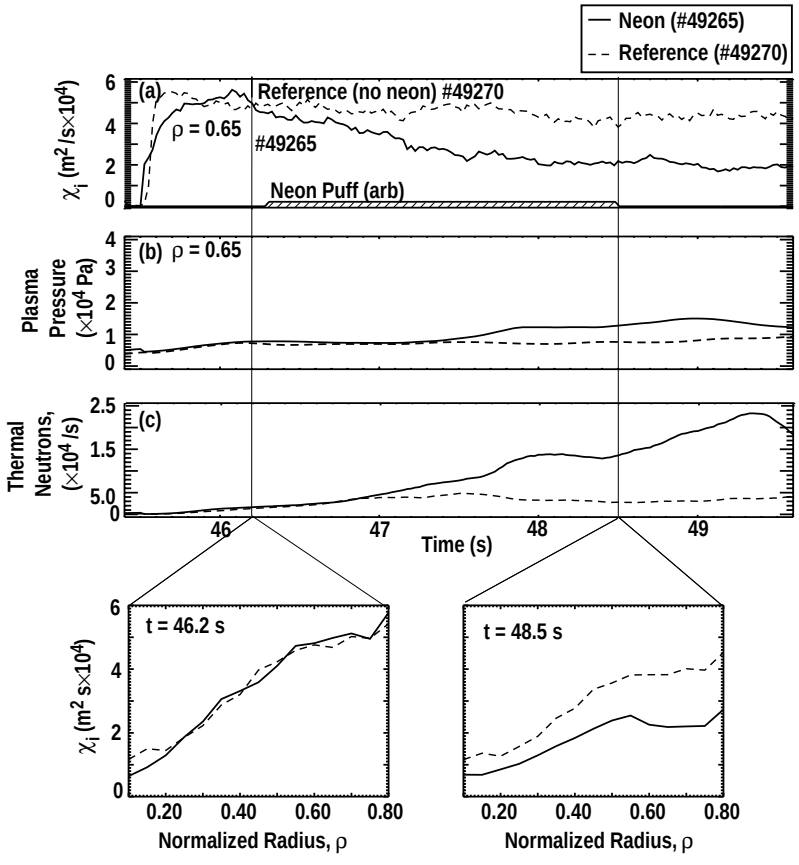

Fig. 2. (a) Ion thermal diffusivity at x=0.65, (b) plasma pressure at x=0.65, and (c) thermal neutron rate for two discharges: #49265 (solid lines) with neon seeding and a reference discharge, #49270 (dashed lines). Profiles χ_i are also shown at two times: 46.2 and 48.5 s.

The γ_{max}/k^2 profiles at three times are plotted in Fig. 4. At 46.2 s, Figs. 4(a) and 4(d) (before neon injection in #49265) ITG turbulence has the highest normalized growth rate and within the uncertainties, the magnitude is comparable for both discharges. At 48.5 s, Figs. 4(b) and 4(e) (the end of the neon puff in #49265)

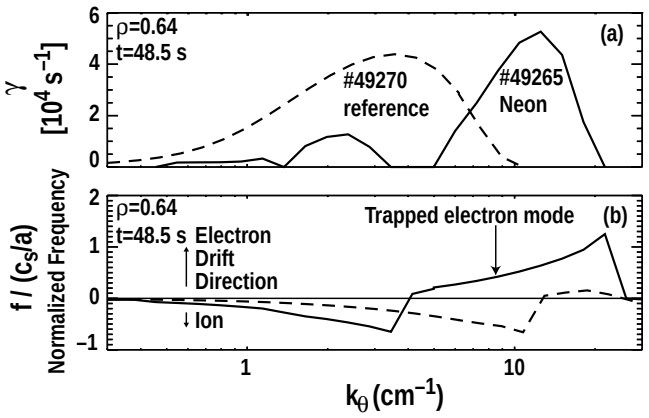

Fig. 3. GKS code growth rate calculations at t=48.5 s and x=0.64 (a) for neon (solid lines) and, reference (dashed lines) discharges described in Fig. 2. Frequencies are displayed in (b).

the trapped electron mode is dominant for $\rho>0.5$, while ITG mode turbulence continues to produce the largest γ_{max}/k^2 in the reference discharge. Comparing the low k spectrum in Fig. 3 at this time, ITG mode turbulence ($f<0$) in the mantle region, $x=0.65$, is significantly reduced. At t=49.4 s, Figs. 4(c) and 4(f) (the neon afterglow phase of #49265) the trapped electron mode growth rate is decreasing over much of the mantle while ITG mode turbulence in the reference discharge remains high. No data is plotted for the neon discharge in Fig. 4(f) for $\rho<0.5$ due to the large uncertainties in the analysis, but qualitatively the maximum normalized growth rate is from ITG turbulence and is much lower than the reference discharge.

The reduction in TE mode growth rates during the neon afterglow, along with the continuing low values of ITG growth rates, may explain the continuing rise in stored energy and H_{89P} observed in many JET discharges after the end of the neon puff.

In these first JET L–mode experiments with impurity injection, modest confinement improvements, $H_{89P} \leqq 1.4$, have been obtained while confinement enhancements up to 2.0 have been observed in DIII–D [3]. Similarities and differences between these two tokamaks are compared in Table 1. Although the impurity injection rate is significantly higher in JET, the fraction of radiated power is not as high as observed in DIII–D. Another difference is that the effects of impurity injection, i.e., increases in P_{rad} n_e, confinement, and thermal neutron rate are prompt in DIII–D, while they are significantly delayed in JET, even after accounting for the delay in the introduction of the neon gas. In addition to size, there are several additional differences between the two tokamaks namely B_T, P_{NB}/V_{plasma}, ∇B drift direction, and toroidal rotation. The combination of TE modes in JET and higher toroidal field may explain the differences in performance between JET and DIII–D. The working hypothesis for DIII–D

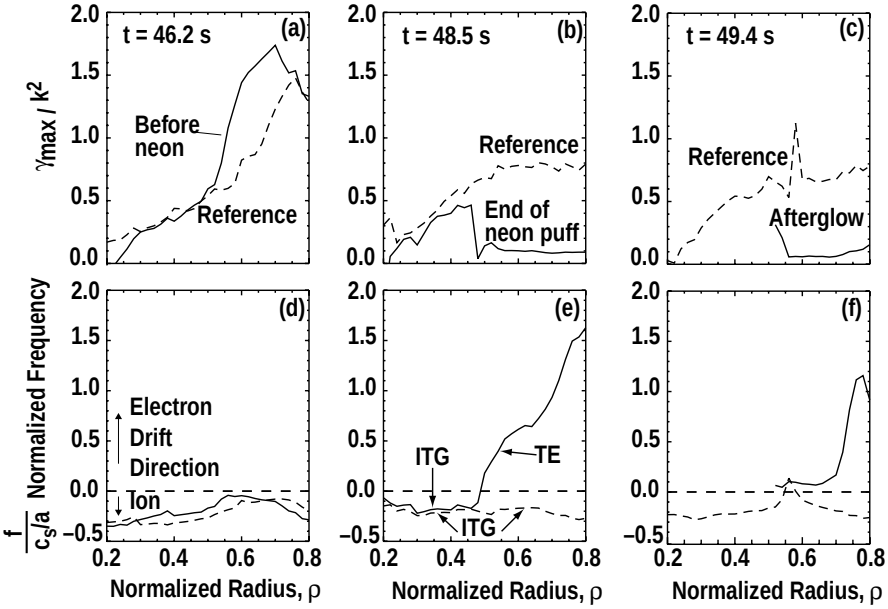

Fig. 4. Maximum growth rate profiles (a), (b), and (c) at three times for discharges described in Figs. 2 and 3. The frequencies, (d), (e), and (f) are also plotted. Solid lines are #49265 and dashed lines are #49270.

is that neon is a trigger causing a decrease in the growth rate of turbulence, leading to improved transport and a larger **E**×**B** shearing rate which, in turn, further stabilizes microturbulence creating a positive feedback loop. The higher toroidal field in these JET discharges, and the lower normalized beam power, P_{NB}/V_{plasma}, may reduce the **E**×**B** shearing rate. This, along with the presence of TE modes, could lead to reduced performance enhancements. We note that decreases in H_{89P} in DIII–D have recently been observed as the toroidal field was increased from 1.6 to 2.0 T [6].

Table 1
Comparison of DIII–D and JET L–mode Discharges with Neon

	DIII–D	**JET**
Plasma volume	20 m^3	80 m^3
Divertor configuration	Upper single null	Lower single null
∇B×B drift direction	Away from X–point	Toward X–point
B_T (typ)	1.6 T	3.0 T
q_{95} (typ)	3.6	4.0
H_{89P} (max)	2.0 (in L–mode)	~1.4 (in L–mode)
$n_e/n_{Greenwald}$	0.5	0.25
P_{rad}/P_{in}	0.7 (typ)	0.6 (max)
P_{nb} (typ)	4.6 MW	5.0 MW
V_ϕ increase after neon?	Yes	No
Largest reduction in thermal diffusivity	ions	ions

In summary, L–mode diverted discharges with neon seeding in JET have been obtained with radiated power fractions, $P_{rad}/P_{in} \leqq 0.6$, confinement enhancements, H_{89P}, up to 1.4, small increases in density, qualitatively similar to, but lower than results obtained in TEXTOR and DIII–D. GKS modeling for JET discharges indicates that with impurity seeding ITG mode growth rates are reduced, but trapped electron modes growth rate increases, which is not seen in other tokamaks. One reason for the differences between JET and other tokamaks with impurity injection into L–mode discharges may be the higher toroidal field and lower toroidal momentum input from neutral beams. Experiments in JET are planned at lower toroidal field and higher beam toroidal momentum input to examine these differences.

Work supported by U.S. Department of Energy under Contract Nos. DE-AC03-99ER54463 and DE-AC02-76CH03073, DE-AC05-00OR22725 and Grant No. DE-FG02-92ER54139.

[1] J. Ongena *et al.*, Plasma Phys. Control. Fusion **41** A379 (1999).
[2] R.J. Goldston *et al.*, J. Comput. Phys. **43**, 61 (1981).
[3] G.R. McKee *et al.*, Phys. Plasmas **7**, 1870 (2000).
[4] R.E. Waltz and R.L. Miller, Phys. Plasmas **6**, 4265 (1999).
[5] M.Z. Tokar *et al.*, Plasma Phys. Control. Fusion **41**, B317 (1999).
[6] M. Murakami *et al.*, "The Physics of Confinement Improvement with Impurity Seeding in DIII–D," to be presented at 27th EPS Conf. on Controlled Fusion and Plasma Physics, June 6–12, 2000, Budapest, Hungary; to be published in the Proceedings.
[7] G.L. Jackson *et al.*, submitted to Nucl. Fusion (2000).